

# Field Construction and Mechanistic Performance of Hot Mix Asphalt Containing Reclaimed Asphalt Pavement

Pranshoo Solanki<sup>1+</sup>, Musharraf Zaman<sup>2</sup>, David Adje<sup>2</sup>, and Zahid Hossain<sup>2</sup>.

**Abstract:** This study explored the potential of using high reclaimed asphalt pavement (RAP) content with hot mix asphalt (HMA) in base and surface courses. A total of four Superpave mixes containing different percentages of RAP namely, 25% RAP and 40% RAP for S3 base courses and 0% RAP and 10% RAP for S4 surface courses were designed, constructed and tested. The mechanistic characteristics of mixes were evaluated by conducting creep compliance, dynamic modulus, Hamburg rut, and 4-point beam fatigue tests. The creep compliance results showed reduction in compliance of the mix due to increase in the RAP content. The dynamic modulus test results illustrated that the asphalt mix containing a higher amount of RAP has higher dynamic modulus values. The increase in RAP content reduced rutting susceptibility and improved moisture damage potential of both S3 and S4 mixes.

DOI:10.6135/ijprt.org.tw/2013.6(4).403

**Key words:** Creep compliance; Dynamic modulus; Fatigue; Moisture damage; Mechanistic; Reclaimed asphalt pavement.

## Introduction

Hot mix asphalt (HMA) is the most widely used paving material in the United States. Each year as much as 100 million tons of HMA are reclaimed during road resurfacing and widening projects. About 80 million tons (80%) are reused as reclaimed asphalt pavement (RAP). Although RAP has been used in the U.S. for over 25 years, with increased environmental awareness and focus on recycling, its enhanced use in pavement construction has become a topic of national importance [1]. In Oklahoma, the current state-of-practice is to allow up to 25% RAP for base courses, but none for surface courses. The current usage of RAP in roads of Oklahoma is significantly lower than the maximum allowable limit and much lower than its neighboring states [2]. Some of the reasons for using a low percentage of RAP in Oklahoma are variations in RAP quality and lack of field/laboratory data on mixes with high RAPs (>25%) [3]. Additionally, the implementation of the Mechanistic-Empirical Pavement Design Guide (MEPDG) requires mechanistic input parameters for asphalt mixes with high RAP [4]. The mechanistic characteristics of new mixes are expected to change as a result of the aged binder and old aggregates introduced to the mix as a part of the RAP.

Many studies have been done to evaluate the effect of RAP on the performance of HMA. Daniel and Lachance [5] examined the effect of increased RAP content on the creep compliance and dynamic modulus of HMA mixes. The compression creep compliance master curves for the control mix and mixes containing 15%, 25%, and 40% processed RAP were developed. The addition of 15% RAP was found to increase the stiffness of the mix and decrease the

compliance, as expected. These results indicated that the mix containing RAP will be more resistant to rutting and less resistant to fatigue fracture and thermal cracking than its virgin counterpart. The mixes containing 25% and 40% RAP, however, did not follow the expected trend. Instead, creep compliance curves were similar to that of the control mix. The results of dynamic modulus of the processed RAP mixes increased from the control (0% RAP) to 15% RAP level, while the 25% and 40% RAP mixes had dynamic modulus curves similar to the control mix. However, no attempt was made to study the effect of RAP content on rutting and moisture damage susceptibility of mixes.

Richardson and Lusher [6] measured the creep compliance of HMA containing 0%, 10% and 20% RAP for surface course mixes in Missouri. The mixes were tested at three different levels of percent air voids (4%, 6.5%, and 9%). Trends such as increasing creep compliance and decreasing tensile strength with increasing percentage of air void and/or temperature were reported. It was found that the presence of RAP in a mix tends to decrease the creep compliance (increase the stiffness) of similar mixes without RAP.

McGraw et al. [7] examined the effect of RAP on dynamic modulus of HMA. A total of 17 mixes containing various amounts of RAP (0%, 10%, 15%, 25% and 30%) were used in this study with two types of binders (PG 58-28 and PG 52-34). It was found that the dynamic modulus increases with increasing RAP content and the differences are more pronounced at lower frequencies (high temperatures). The increase in dynamic modulus was noticeably higher in the mix containing 30% RAP than that of the control mix (0% RAP).

Loria et al. [8] evaluated the dynamic modulus of HMA mixes containing RAP (15% and 50%). The dynamic modulus values were found to increase with the increase in RAP content. However, a reduction in the dynamic modulus was observed for the mixes containing 50% RAP and PG 52-34 as compared to mixes containing 50% RAP and a PG 58-28 binder. It was also found that the field-produced mixes exhibited significantly higher dynamic modulus values than the comparable laboratory-produced mixes, except for the field and laboratory-produced mixes containing 0%

<sup>1</sup> Department of Technology, Illinois State University, Campus Box 5100, Normal, IL 61790, USA.

<sup>2</sup> School of Civil Engineering and Environmental Science, University of Oklahoma, Norman, OK 73019, USA.

<sup>+</sup> Corresponding Author: E-mail psolanki@ilstu.edu

Note: Submitted January 25, 2013; Revised June 26, 2013; Accepted June 27, 2013.

and 50% RAP. Both studies (McGraw et al., 2010; Loria et al., 2011) were limited to the evaluation of dynamic modulus.

Bonaquist [9] examined the creep compliance of 16 Wisconsin mixes. Of these, eight mixes were virgin containing different types of aggregate and the remaining eight mixes included 25% recovered RAP binder. A total of two types of binder, namely, PG 58-28 and PG 58-34, were used. It was found that the low temperature creep compliance is a function of only the low temperature compliance of the mixes tested. Aggregate source and design traffic level did not show any significant effect on the low temperature compliance of the mixes. Also, it was reported that the measured compliance values are higher than the predicted MEPDG Level 3 compliance values with errors as high as 56%. This level of error necessitates actual measurement of creep compliance values. It is also worth mentioning here that the RAP containing mixes in this study were prepared by extracting and recovering RAP binder from a single Wisconsin source, then replacing 25% of the binder in each mix with the recovered RAP binder. The method used in this study for recovering binder from RAP and mixing it in the virgin mix is not representative of the field conditions.

Rahman et al. [10] evaluated rutting susceptibility of mixes containing RAP by conducting Hamburg wheel-tracking tests. It was found that the rutting performance was significantly affected by the asphalt binder source and grade regardless of RAP content. The surface mixes with higher RAP content were found not significantly susceptible to rutting compared to the mixes with moderate RAP contents. No further attempt was made to evaluate creep compliance and dynamic modulus which are important parameters for mechanistic design of pavements [4].

In a recent study, Silva et al. [11] produced totally recycled HMA mixes, i.e., HMA mixes containing 100% RAP. The performance of totally recycled HMA mixes was evaluated by conducting water sensitivity, rutting resistance, stiffness, fatigue resistance, and binder aging tests. It was found that the totally recycled HMAs can be a good alternative with performance as good as conventional HMAs, provided that adequate storing and handling conditions are assured during the production stage.

In another recent study, Singh et al. [12] investigated effect of long-term oven aging on RAP mixes using dynamic modulus test. It was found that long-term oven aging increased dynamic modulus of the compacted samples by 42% to 60%, depending on the amount of RAP and air void content of the compacted specimen. However, no attempt was made to evaluate other relevant pavement performance parameters.

Although some of the aforementioned studies are relevant to this research [e.g., 11], it is also important to note that the mineralogical and chemical characteristics of RAP and virgin aggregates and binders in Oklahoma are different than those in other regions, and thus results from other studies may not be directly used for the design of pavements in Oklahoma at a Level 1 or Level 2 design [4]. Consequently, the current study explores the effect of different RAP contents on the mechanistic characteristics of HMA by conducting creep compliance, dynamic modulus, Hamburg rut, and 4-point beam fatigue tests. A total of four Superpave mixes containing different percentages of RAP namely, 25% RAP and 40% RAP for Oklahoma S3 base courses and 0% RAP and 10% RAP for

Oklahoma S4 surface courses were designed, constructed and tested.

## Materials and Methods

### Materials

The RAP was selected with the help of Silver Star Construction Co. located in Moore, OK. The location of the RAP source was I-35 in McClain County (near Purcell), Oklahoma. The RAP milling site had a 37 mm (1.5 in.) overlay of HMA Type B with PMAC-1C binder in 1994. Before 1994, the project had received a 50 mm (2 in.) leveling course of HMA Type C with AC-3 (viscosity grading) binder back in 1979. In addition to the collection of RAP millings, four different types of virgin aggregates, namely, #67 Rocks, 5/8-in. chips, screenings, manufactured sand, and natural sand, and a virgin binder (PG 64-22 OK from Valero at Ardmore, Oklahoma) were collected for mix design and laboratory testing.

### Volumetric Mix Design

As noted earlier, a total of four mixes, namely, S3 mix containing 25% RAP (S3-25), S3 mix containing 40% RAP (S3-40), S4 mix containing 0% RAP (S4-0), and S4 mix containing 10% RAP (S4-10), were prepared. Several trials were attempted where the percentages of blended materials for fulfilling the consensus properties and volumetric mix design requirements were changed in accordance with the Superpave requirements (AASHTO M 323) and test procedures (AASHTO R 35). Volumetric properties recommended specifically, bulk specific gravity ( $G_{mb}$ ) (AASHTO T 166), maximum specific gravity ( $G_{mm}$ ) (AASHTO T 209) void in mineral aggregates (VMA), void filled with asphalt (VFA), and dust-to-binder ratio were determined with different binder content. The S3 and S4 mixes were designed for a design equivalent single axle load (ESAL) value of 0.3 M – 3 M.

### Test Site Description

The test site for this study was selected in cooperation with Silver Star Construction Co. in Moore, Oklahoma and is located on York Drive near US 77 in Norman, Oklahoma (Fig. 1(a)). The test site is a two-lane city road having a length of approximately 204 meter (670 ft). Prior to paving, the existing silty clay subgrade was stabilized with 14% Cement Kiln Dust (CKD) (Fig. 1(b)).

### Construction of South Lane (S3-25 and S4-0 Mixes)

The south lane of the test section was constructed with a S3-25 mix, overlaid by a S4-0 mix (current state of practice). The paving machine was equipped with an electronic slope and grade control. The S3-25 layer was constructed in two lifts, each having a thickness of 72 mm (3 in.). After the laydown of the first lift (Fig. 1(c)), it was compacted by using a vibratory compactor with steel drum roller (CAT PS-360B) (Fig. 1(d)). The rolling pattern was decided on the basis of density readings obtained from a nuclear density gage. Both density and temperature were recorded for each pass until the density started decreasing with the number of passes.



**Fig. 1.** (a) Right of Way (Natural Subgrade), (b) Mixing CKD With Subgrade, (c) Laydown of S3-25 Layer (South Lane), (d) Compaction of S3-25 Layer With Steel Drum Roller, (e) Compaction of S3-25 Layer With Rubber-tire Roller, (f) Laydown of S4-0 Layer (South Lane), (g) Placement of Paper During Laydown of S4 Layers, and (h) Laydown and Compaction of S4-0 Layer (South Lane).

During the trial compaction, it was found that three and a half passes were required to achieve the desired level of compaction. Therefore, it was decided to use only three passes for compaction. Following the vibratory compaction, a rubber-tire roller DYNAPAC CA-251 (Fig. 1(e)) was used to smoothen the surface. A total of five passes were made using this rubber-tire roller. Finally, the vibratory compactor (CAT PS-360B) was used again without any vibration for finish rolling. Only one pass was used this time. After the construction of the first lift, its thickness was determined by taking three cores and measuring the thickness of each core. The thicknesses of these cores were 79.0 mm (3.1 in.), 74.8 mm (2.9 in.) and 76.4 mm (3.0 in.), with an average thickness of 76.2 mm (3 in.). Henceforth, the same amount of mix (135 tons of material) was used to achieve the next 76.2 mm (3 in.) of the second lift. The second lift of S3-25 layer was constructed using the same equipment and procedure as outlined above for the first lift.

After the construction of S3 layers, a tack coat (SS-1HP) was sprayed on the S3 layer before the construction of the S4 layers. The south lane of the test section was constructed with S4-0 mix (Fig. 1(f)). During the paving of the S4-0 layer, paper was placed between the S3-25 and S4-0 layers at selected locations for the ease of extracting cores (Fig. 1(g)). Further after paving, those selected locations were labeled by using spray paint on the top of the S4-0 layer. After laydown, compaction was conducted using a vibratory compactor with steel drum (CAT PS-360B) (Fig. 1(h)). As before, the rolling pattern was decided on the basis of density readings obtained from a nuclear density gage during trial rolling. Both density and temperature were recorded for each pass until the density started decreasing with the number of passes. It was found that approximately four passes are enough to achieve the desired level of compaction.

#### ***Construction of the North Lane (S3-40 and S4-10 Mixes)***

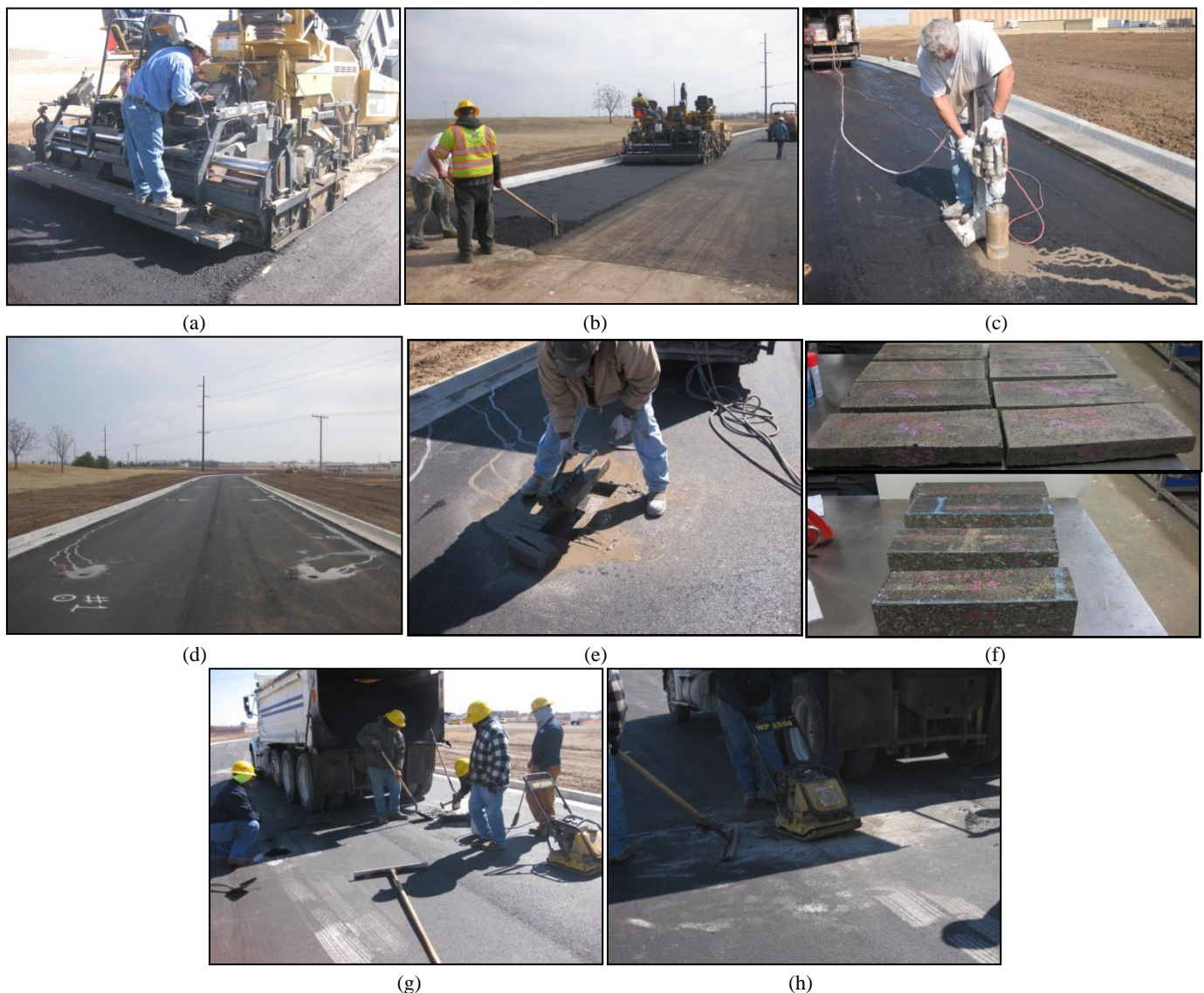


**Fig. 2.** (a) Laydown of S3-40 Layer (North Lane), (b) Laydown of S4-10 Layer over S3-40 Layer (North Lane), (c) Coring Operation S3-25 (South Lane), (d) Core Locations, (e) Extraction of Block Samples, (f) Extracted Surface and Base Course Blocks, (g) Patching Process of the Holes, and (h) Plate Compaction During Patching Holes.

The north lane of the test section was constructed using the same equipment and procedure as outlined above for the south lane. This lane was constructed with a S3-40 mix overlaid by a S4-10 mix, and four passes were used to achieve the desired level of compaction for S3-40. The thickness of the first lift of S3-40 mix (Fig. 2(a)) was determined by taking three cores and measuring the thickness of each core. It was found that thicknesses of the cores are 79.0 mm (3.1 in.), 74.8 mm (2.9 in.) and 76.4 mm (3.0 in.) with an average thickness of 76.2 mm (3.1 in.). Henceforth, the same amount of mix (135 tons of material) was used to achieve the next 76.2 mm (3.0 in.) of the second lift. After the construction of S3-40 layers, the S4-10 layer (Fig. 2(b)) was constructed. Five passes were used to achieve the desired level of compaction for this layer.

#### ***In Situ Coring and Block Sample Extraction***

The in situ coring and extraction of block samples was first

performed on February 24, 2011, after the construction of the base layers and again on February 28, 2011, after the construction of the surface layers. A total of eighteen cores and four blocks were extracted from the base layers, while fourteen cores and eight blocks were retrieved from surface layers. The location, the mix type and the thickness of all the cores is presented in Table 1. The cores were extracted at a regular interval of 15.2 meter (50 ft) and 23 meter (75 ft) from each other for the base and surface layers, respectively. The core specimens were retrieved from both lanes between the expected wheel paths, as shown in Fig. 2(c) and 2(d). As shown in Fig. 2(d), cores of same diameter 152 mm (6 in.) were obtained. Each core was taken to full depth of the asphalt pavement layer. The average thicknesses of the cores were 158 mm (6.222 in.), 152.4 mm (6.0 in.), 80.28 mm (3.161 in.), and 79.38 mm (3.125 in.) for S3-25, S3-40, S4-0, and S4-10, respectively. One of the reasons for lower layer thickness of higher RAP containing mixes (S3-40 and S4-10) as compared to corresponding lower RAP containing mixes

**Table 1.** Summary of Location and Thickness of Core Specimens Retrieved from the Test Sections.

Cores from S3 Layers				Cores from S4 Layers			
Core #	Distance from west end (ft)	Mix Type	Thickness (in.)	Core #	Distance from West End (ft)	Mix Type	Thickness (in.)
1	50	S3-25	5.875	1	75	S-4-0	3.125
2	100	S3-25	5.625	2	112	S-4-0	3.25
3	150	S3-25	5.75	3	171	S-4-0	3.125
4	200	S3-25	6.375	4	208.5	S-4-0	3.25
5	250	S3-25	6.25	5	325	S-4-0	3.125
6	300	S3-25	6.875	6	464	S-4-0	3.125
7	350	S3-25	6.625	7	595.6	S-4-0	3.125
8	400	S3-25	6.375	8	103	S-4-10	2.5
9	450	S3-25	6.25	9	191	S-4-10	3
10	50	S3-40	6	10	267	S-4-10	3.125
11	100	S3-40	5.625	11	387.5	S-4-10	3.125
12	150	S3-40	5.625	12	458.7	S-4-10	3.25
13	200	S3-40	5.875	13	522.6	S-4-10	3.625
14	250	S3-40	5.625	14	608.3	S-4-10	3.25
				Average Layer Thickness (from Cores)			
15	300	S3-40	6	S3-25 = 6.222 in. (158 mm)			
16	350	S3-40	6.5	S3-40 = 6.000 in. (152.4 mm)			
17	400	S3-40	6.75	S4-0 = 3.161 in. (80.28 mm)			
18	450	S3-40	6	S4-10 = 3.125 in. (79.38 mm)			

(S3-25 and S4-0) could be higher number of passes used for compaction of S3-40 (four passes) and S4-10 (five passes) layers.

After extraction, the cores were properly labeled and carefully wrapped so that they can be brought to the laboratory in good condition. Each block sample was approximately 457 mm (18 in.) long and 178 mm (7 in.) wide. The block samples were extracted using a concrete saw-cutting machine at regular interval of 52 meter (170 ft) and 40 meter (132 ft) from each other for the base and surface layers, respectively (Fig. 2(e)). All block samples were labeled and carefully transported to the laboratory on a hard support to prevent bending (Fig. 2(f)). After extraction, Silver Star Construction patched all the holes with HMA, followed by compaction with a plate compactor, as shown in Fig. 2(g) and 2(h).

### Specimen Preparation

The field cores were further saw-cut in the laboratory to a diameter of 150±9 mm (6±0.35 in) and thickness (height) of 45 mm (1.8 in.) in preparation for creep compliance testing. In this study, the field cores tested for creep compliance had an air void content of 6±0.5% in accordance with the OHD L-45 test method [13]. The plant mixes were used to prepare specimen at a target air void content of 7±0.5% using a Superpave gyratory compactor (AASHTO T 312) for dynamic modulus testing. The selected field cores of S4 and S3 mixes were saw-cut to a diameter of 150 mm (6 in.) and a height of 60±2 mm (2.36±0.08 in.) for conducting Hamburg rut tests. Each block sample was saw-cut into two beams (length = 15 in; width = 2.5 in; height = 2 in) for 4-point beam fatigue testing.

### Creep Compliance

Creep compliance is defined in AASHTO T 322 as “the time-dependent strain divided by the applied stress.” In this study,

creep compliance tests were conducted at -18°C, -10°C, 0°C, and 10°C on cylindrical cores (diameter = 150 mm, height = 45 mm) in accordance with the AASHTO T 322 test method. The test method consists of the application of a static load of fixed magnitude along the diametral axis of a specimen for 100 seconds. A 100 kN (22,000 lb) load cell was used for loading the specimen. The vertical and horizontal deformations were measured by two LVDTs having a stroke length of 5 mm (0.2 in.), attached in the diametrically perpendicular direction. A gauge length of approximately 38 mm (1.5 in.) was used for mounting LVDTs on one face of the specimen. The horizontal and vertical deformations measured near the center of the specimen were used for calculating the tensile creep compliance as a function of time. The applied load was selected to keep horizontal deformation in the linear viscoelastic range (0.012 – 0.019 mm, 0.000492 – 0.0007480 in.) during the creep test. Following AASHTO T 322 test method guidelines, creep compliance was calculated using the following equation:

$$D(t) = \frac{\Delta X_{m,t} D_{avg} b_{avg}}{P_{avg} GL} C_{cpl} \quad (1)$$

where,  $D(t)$  = creep compliance at time  $t$ ,  $GL$  = gauge length in inches (38 mm, 1.5 in.),  $D_{avg}$  = average diameter of the specimen,  $b_{avg}$  = average thickness of the specimen,  $\Delta X_{m,t}$  = trimmed mean of the normalized, horizontal deformations (nearest to 0.02 mm, 0.001 in.) for faces of the specimen at time  $t$ ,  $P_{avg}$  = average creep load (N, lb),  $C_{cpl}$  = correction factor defined as:

$$C_{cpl} = 0.6354 \left( \frac{X}{Y} \right)^{-1} - 0.332 \quad (2)$$

where,  $X/Y$  = absolute value of the ratio of the normalized, trimmed mean of the horizontal deformations ( $\Delta X_{m,t}$ ) to the normalized, trimmed mean of the vertical deformations ( $\Delta Y_{m,t}$ ) at a time

corresponding to  $\frac{1}{2}$  of the total creep compliance test time. The restrictions of the correction factor (Eq. (2)) are given by the following equation:

$$\left[ 0.704 - 0.213 \left( \frac{b_{avg}}{D_{avg}} \right) \right] \leq C_{cpl} \leq \left[ 1.566 - 0.195 \left( \frac{b_{avg}}{D_{avg}} \right) \right] \quad (3)$$

The master creep compliance curve was created using the time-temperature superposition principle; the time and temperature-dependent material properties can be represented by using reduced time ( $t_r$ ) [6]. For a constant temperature, the reduced time ( $t_r$ ) is defined as:

$$t_r = t \times a_t \quad (4)$$

where,  $a_t$  = time-temperature shift factor, and  $t$  = time (seconds). A template developed in an MS Excel spreadsheet was used to generate a master creep compliance curve by shifting the creep compliance values as a function of time data at each temperature to a reference temperature of  $-18^\circ\text{C}$ . This was achieved by numerical optimization using Eq. (5) to model the master creep compliance curve of the mix [13], as shown below:

$$D(t) = D_0 + D_1 \left( \frac{t}{10^{C_2(T_r - T)}} \right)^m \quad (5)$$

where,  $D_0$ ,  $D_1$ ,  $m$  = fitting parameters,  $C_2$  = time-temperature shift constant,  $T_r$  = reference temperature, and  $T$  = temperature. To compare the master curves, creep compliance values were calculated from the fitted master curves over the range of reduced times used in the AASHTO T 322 testing, which is from approximately 1 to 100,000 seconds.

Further, Poisson's ratio ( $\nu$ ) values were calculated using Eq. (6) in accordance with AASHTO T 322 test method, as shown below:

$$\nu = -0.10 + 1.48 \left( \frac{X}{Y} \right)^2 - 0.778 \left( \frac{b_{avg}}{D_{avg}} \right) \left( \frac{X}{Y} \right)^2 \quad (6)$$

## Dynamic Modulus

The dynamic modulus (AASHTO TP 62) testing was done at five different temperatures  $-10^\circ\text{C}$ ,  $4.4^\circ\text{C}$ ,  $21.1^\circ\text{C}$ ,  $37.8^\circ\text{C}$ ,  $54^\circ\text{C}$  ( $14^\circ\text{F}$ ,  $40^\circ\text{F}$ ,  $70^\circ\text{F}$ ,  $100^\circ\text{F}$  and  $130^\circ\text{F}$ ) starting at the lowest temperature and proceeding to the highest temperature. For each temperature level, test was run at six different frequencies from the highest to lowest, including 25 Hz, 10 Hz, 5 Hz, 0.5 Hz, 0.1 Hz. The master curves for S3-25 and S3-40 mixes were generated at a reference temperature of  $21.1^\circ\text{C}$  ( $70^\circ\text{F}$ ) using the procedure outlined in [14]. Additional details of testing methodology and analysis are presented elsewhere [3].

## Hamburg Rut Testing

For determining rut and moisture damage (stripping), cores were tested by using Hamburg wheel-tracking machine in accordance

with OHD L 55 test method [15]. Susceptibilities to rutting and moisture are based on pass/fail criteria [15]. The test requires cores secured in mounting tray using plaster of Paris. During testing the 47 mm (1.85 in) wide wheel is tracked across a sample submerged in water bath for 20,000 passes or until a rut depth of 20 mm occurs. The load on the wheel is 705 N (158 lb). The temperature of water bath was maintained at  $50 \pm 1^\circ\text{C}$  ( $122 \pm 2^\circ\text{F}$ ). Rut depth was measured continuously with a series of LVDTs on the sample. The LVDT measures the depth of the rut with an accuracy of 0.01 mm. On a typical test result curve, primarily three characteristic regions are generally defined, including post-compaction consolidation, creep slope, stripping slope, and stripping inflection point [16 – 18]. Texas Department of Transportation (TxDOT) has adopted this test and recommended a maximum allowable rut depth of 12.5 mm at 20,000 passes for PG-76 or higher, at 15,000 passes for PG-70 and at 10,000 passes for PG-64 or lower [18]. It is worth mentioning here that the Hamburg wheel-tracking machine has been found to have excellent correlation with field performance [18 – 20]. So, it was decided to conduct this test on mixes as an additional performance indicator.

## 4-point Beam Fatigue Testing

In the present study, beams were tested for fatigue life under 4-point loading inside a beam fatigue apparatus, in accordance with the AASHTO T 321 test method. The advantage of using a 4-point beam fatigue apparatus is that it produces a constant bending moment over the center third span between the H-frame contact points on the beam specimen (ASTM D 7460). This apparatus also allows free rotation and translation at all load and reaction points. The fatigue life tests consist of applying a repeated constant vertical strain to a beam specimen in flexural tension mode until failure or up to a specified number of load cycles. In this test, the input strain was sinusoidal shaped, applied at a frequency of 10 Hz in accordance with the AASHTO T 321 test method. The test was conducted at a strain level of 200 microstrain, consistent with the AASHTO T 321 test method recommendations for conventional HMA. Failure is assumed to occur when the stiffness reached half of its initial value, which is determined from the load at 50th cycle. The fatigue life ( $N_f$ ) is the total number of load repetitions that cause a 50 percent decrease in initial stiffness (AASHTO T 321). The test is terminated manually when the initial stiffness has diminished by 50 percent or when a preset number of load cycles (2,000,000) is reached. The flexural stress, strain and stiffness of beams were determined by using the following expressions (AASHTO T 321):

$$\sigma_f = \frac{3aP}{bh^2} \quad (7)$$

$$\varepsilon_f = \frac{12\delta h}{(3L^2 - 4a^2)} \quad (8)$$

$$M_{ff} = \frac{\sigma_f}{\varepsilon_t} = \frac{aP(3L^2 - 4a^2)}{4b\delta h^3} \quad (9)$$

where  $\sigma_f$  = tensile stress at the bottom of beam,  $\varepsilon_t$  = tensile strain at

the bottom of beam,  $M_r$  = flexural stiffness,  $P$  = applied peak load,  $a$  = spacing between inside clamps (119 mm, i.e., 4.69 in),  $b$  = average beam width,  $h$  = average beam height,  $\delta$  = beam deflection in neutral axis,  $L$  = length of beam between outside clamps or supports (35.56 mm, i.e., 14 in). In this study, a total of six beam specimens were tested at a temperature of 20°C (68°F). It is important to note that the total number of beams tested in this study were actually more than six. However, some of the beams fractured during saw-cutting or before conducting test and some beams fractured along the clamp edge at 400 microstrain while conducting test. Thus, these beams were disregarded and not considered further in this study.

## Presentation and Discussion of Results

### Volumetric Properties

The percentage of materials and corresponding gradations, and volumetric properties of the final S3 and S4 mixes are presented in Table 2(a) and 2(b), respectively. The S3-25 and S3-40 mixes (Table 2(a)) are blend of different percentages of 5/8-in chips, screening, and manufactured sand. Similarly, the S4-10 mix (Table 2(b)) is a blend of 5/8-in chips, screening, manufactured sand and natural sand. Both S3 and S4 mixes are well within the limits of the

gradation, as recommended by AASHTO M 323. It is also evident from Table 2(a) and 2(b) that the voids in mineral aggregate (VMA) and voids filled with asphalt (VFA) values increase with the amount of RAP. Overall, the VMA and VFA increased by 1.7% and 6.4%, respectively, due to increase in RAP by 15% (from 25% to 40%) for S3 mixes. Similarly, the VMA and VFA increased by 0.1% and 3.7%, respectively, due to increase in RAP by 10% (from 0% to 10%) for S4 mixes. This could be attributed to the difference in the extent of blending of the RAP material with the virgin materials [5]. If the RAP material is not heated sufficiently, the RAP binder does not blend with the virgin binder and the RAP tends to act more like a black rock material. The incomplete blending of RAP material with virgin material will produce coarser gradation of the overall mix resulting in more compaction effort and increased VMA [5].

### Creep Compliance and Poisson's Ratio

The master curves for creep compliance were generated for both S3-25 and S3-40 mixes, as well as for both S4-0 and S4-10 mixes as shown in Fig. 3. It is clear from Fig. 3 that S3-25 mixes showed lower creep compliance values as compared to S3-40 mixes up to a reduced time of 10 seconds (low temperature). Beyond 10 seconds, S3-25 mixes start showing higher creep as compared to the S3-40 mix. Also, differences in creep values between the S3-25 and S3-40

**Table 2.** (a) Gradation and Volumetric Properties of S3 Mixes.

Blended Material	S3-25	S3-40	Gradation (Sieve Size, mm)	% Passing		Required <sup>2</sup>
				S3-25	S3-40	
# 67 Rock	15%	12%	25	100	100	100
5/8" Chips	22%	25%	19	99	97	90-100
Sreenings	17%	8%	12.5	89	90	≤ 90
Manufactured Sand	10%	15%	9.5	78	70	-
Natural Sand	11%	0%	4.75	56	43	-
RAP	25%	40%	2.36	39	24	23-49
			1.18	31	16	-
			0.6	25	11	-
			0.3	18	7	-
			0.15	9	5	-
			0.075	5.2	2.7	2-8
Volumetric Properties			Aggregate Properties for Volumetric Design			
$G_{mm}$	2.533	2.475	LA Abrasion(%)	21	22	≤ 40
$G_{se}$	2.722	2.665	Micro-Deval (%)	11.8	12.5	≤ 25
$G_{sd}$	2.671	2.628	Sand Equivalent (%)	78	82	≥ 40
$G_b$	1.01	1.01	Fine Aggregate Angularity(%)	43.5	42	≥ 40
Virgin Binder Type	PG 64-22	PG 64-22	Mixture Properties for Volumetric Design			
Total Binder Content (%)	4.4	4.7	Tensile Strength Ratio	0.87	0.82	≥ 0.08
Virgin Binder Content (%)	2.9	2.9	APA Rut (mm)	1.1	3.6	≤ 6
VMA (%) (Required: ≥ 13.0)	13.5	15.2	Permeability ( $10^{-5}$ cm/s)	6.4	6.5	≤ 12.5
VFA (%) (Required: 65-78)	67.2	73.6				
DP (%) (Required: 0.6-1.2)	1.1	0.8				

\*Required for 0.3-3M of Design ESAL; RAP: Recycled Asphalt Pavement; S3-25 Mix Containing 25%OAP; S3-40: S3 Mix Containing 40% RAP;  $G_{mm}$ : Maximum Theoretical Specific Gravity;  $G_{se}$ : Effective Specific Gravity of Aggregate;  $G_{sb}$ : Bulk Specific Gravity of Aggregate;  $G_b$ : Specific Gravity of Binder; VMA : Voids in Mineral Aggregates; VFA : Voids Filled With Asphalt; DP : Dust Proportion; APA: Asphalt Pavement Analyzer

**Table 2.** (b) Gradation and Volumetric Properties of S4 Mixes.

Blended Material	S4-0	S4-10	Gradation (Sieve Size, mm)	% Passing		Required <sup>2</sup>
				S4-0	S4-10	
5/8" Chips	25%	30%	19	100	100	90-100
1/2" Chips	18%	0%	12.5	96	98	≤ 90
Sreenings	42%	22%	9.5	88	90	-
Manufactured Sand	0%	33%	4.75	57	68	-
Natural Sand	15%	5%	2.36	35	39	23-49
Fine RAP	0%	10%	1.18	28	25	-
			0.6	23	17	-
			0.3	15	10	-
			0.15	7	6	-
			0.075	4.6	2	2-8
Volumetric Properties			Aggregate Properties for Volumetric Design			
G <sub>mm</sub>	2.488	2.47	LA Abrasion(%)	18	21	≤ 40
G <sub>se</sub>	2.699	2.687	Micro-Deval (%)	7.7	11.8	≤ 25
G <sub>sd</sub>	2.67	2.605	Sand Equivalent (%)	67	75	≥ 40
G <sub>b</sub>	1.01	1.01	Fine Aggregate Angularity(%)	42.7	41.6	≥ 40
Virgin Binder Type	PG 64-22	PG 64-22	Mixture Properties for Volumetric Design			
Total Binder Content (%)	5.1	5.3	Tensile Strength Ratio	0.85	0.82	≥ 0.08
Virgin Binder Content (%)	5.1	4.8	APA Rut (mm)	1.39	4.2	≤ 6
VMA (%) (Required: ≥ 14.0)	15.8	15.9	Permeability (10 <sup>-5</sup> cm/s)	3	10.4	≤ 12.5
VFA (%) (Required: 65-78)	69.6	73.3				
DP (%) (Required: 0.6-1.2)	0.97	0.6				

\*Required for 0.3-3M of Design ESAL; S4-0: Mix Containing 0% RAP; S4-10: Mix Containing 10%RAP; G<sub>mm</sub>: Maximum Theoretical Specific Gravity; G<sub>se</sub>: Effective Specific Gravity of Aggregate; G<sub>sb</sub>: Bulk Specific Gravity of Aggregate; G<sub>p</sub>: Specific Gravity of Binder; VMA : Voids in Mineral Aggregates; VFA : Voids Filled With Asphalt; DP : Dust Proportion; APA: Asphalt Pavement Analyzer

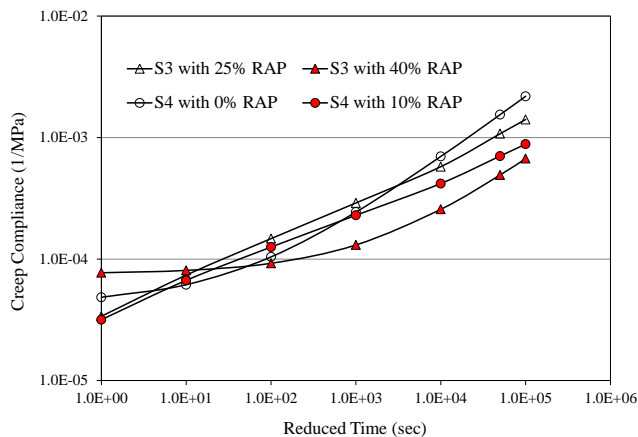


**Fig. 3.** Creep Compliance Master Curves of Mixes.

mixes are more pronounced at higher reduced time or temperature. For example, at a reduced time of 100 seconds, the S3-25 mixes had approximately 60% higher creep compliance values as compared to the S3-40 mix. However, the difference between creep compliance values for the S3-25 and S3-40 mixes increased to 124% at a reduced time of 10,000 seconds. Similar trends were also observed with the S4 mixes; however, the S4-0 mix showed higher creep beyond a reduced time of 1,000 seconds. For example, at a reduced time of 10,000 seconds, the S4-0 mix had approximately 67% higher creep compliance values as compared to the S4-10 mix. The difference of creep compliance values between the S4-0 and S4-10 mixes increased to 148% at a reduced time of 100,000 seconds. This behavior of the S3 and S4 mixes with the increase of RAP content

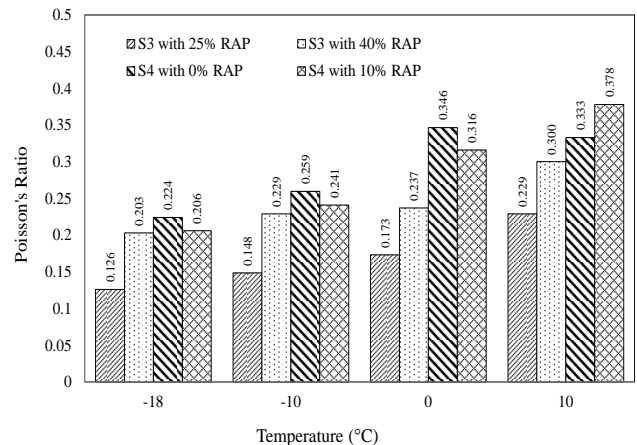


**Fig. 4.** Poisson's Ratio of Mixes.

in the mixes, is consistent with the observations reported by other researchers [5 – 6, 9].

Fig. 4 shows plot of average values of Poisson's ratio for S3 and S4 mixes. It is evident from Fig. 4 that Poisson's ratio values increase with increasing temperature, as expected [6]. The results of the S3 mixes, present an increase in Poisson's ratio values with an increase in the RAP content. For example, at -18°C (-0.4°F), the value of Poisson's ratio increases from 0.127 to 0.208 for the S3-25 and S3-40 mixes, respectively. Comparatively, the results of S4 mixes show a decrease in the Poisson's ratio values with an increase in the RAP content, except for the results at 10°C (50°F). Thus, the RAP content can increase the Poisson's Ratio as it is the case here

for S3 mixes and reported by Richardson and Lusher [6] or decrease the Poisson's Ratio values of the HMA as it is the case here for S4 mixes.

### Dynamic Modulus and Shift Factors

The master curves for S3 mixes (S3-25 and S3-40) and S4 mixes (S4-0 and S4-10) are presented in Fig. 5. From Fig. 5, it is generally evident that the dynamic modulus of the S3-40 mix is higher than that of the S3-25 mix. For example, the S3-40 mix produced dynamic modulus values approximately 35%, 40% and 65% higher at a reduced frequency of  $10^{-7}$ , 1 and  $10^7$  Hz, respectively, as compared to the corresponding S3-25 mix. The same trend is also evident for S4 mixes, where the dynamic modulus of the S4-10 mix is found to be higher than that of S4-0 mix. For example, S4-10 mix produced dynamic modulus values approximately 40%, 35% and 42% higher at a reduced frequency of  $10^{-7}$ , 1 and  $10^7$  Hz, respectively, as compared to the S4-0 mix. This observation is in agreement with previous results reported by other researchers [7, 20 – 21].

The log of shift factors used for developing the master curves of S3 (S3-25 and S3-40) and S4 mixes (S4-0 and S4-10) are presented in Fig. 6. It is evident from Fig. 6 that S3-25 and S3-40 mixes had similar magnitude ( $\pm 0.1$ ) of shift factors up to the reference temperature (21.1°C). Above this reference temperature, S3-40 mix exhibited a higher magnitude of shift factor as compared to the S3-25 mix at a comparable temperature. Below reference temperature, the shift factors for S4 mixes exhibited higher magnitude for mixes with lower percentage of RAP (S4-0). However, shift factors of S4 mixes did not follow any particular trend above reference temperature. Some researchers have reported that the differences between the modulus values due to RAP are more pronounced at higher temperature or lower frequencies [22].

### Hamburg Rut

The test results for S3 mixes are presented in Fig. 7. It is evident from Fig. 7 that the rut depth of S3-25 mix is higher than the rut depth of S3-40 mix. For example, at 10,000 passes S3-25 and S3-40 mixes showed a rut depth of approximately 4.54 and 3.62 mm, respectively. Similar behavior of increase in rut with increase in RAP content is evident for S4 mixes as well (Fig. 7). For example, application of 10,000 passes on S4-0 and S4-10 mixes produced a rut depth of approximately 8.91 and 6.06 mm, respectively. As presented in Fig. 7, all four characteristic regions are evident in S3-25 and S4-0 mixes. The stripping inflection points for S3-25 and S4-0 mixes were found approximately 17,000 and 15,700 passes, respectively. According to FHWA [23], an inflection point below 10,000 wheel passes indicates significant moisture damage susceptibility in the mix. No stripping slope and inflection point was observed in mixes containing corresponding higher percentage of RAP (S3-40 and S4-10).

### 4-point Beam Fatigue

Table 3 summarizes the test matrix and air void content of each specific beam. Test data were analyzed using Eqs. (7) through

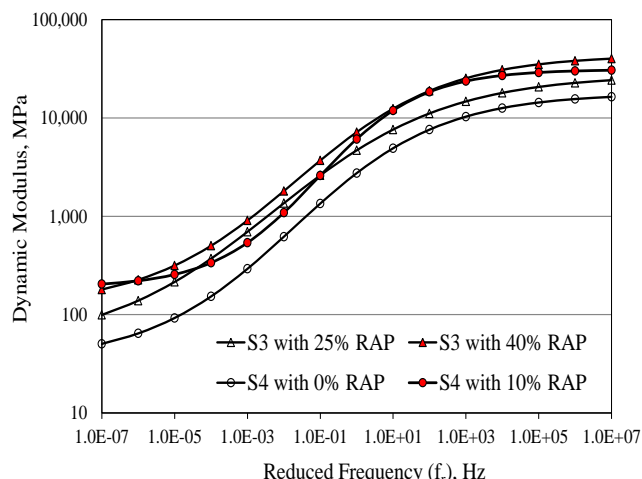


Fig. 5. Dynamic Modulus Master Curves of Mixes.

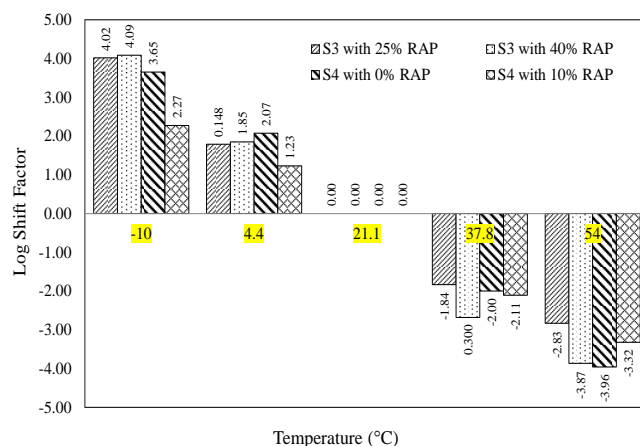


Fig. 6. Comparison of Shift Factors Used for Generating the Dynamic Modulus Master Curves of Mixes.

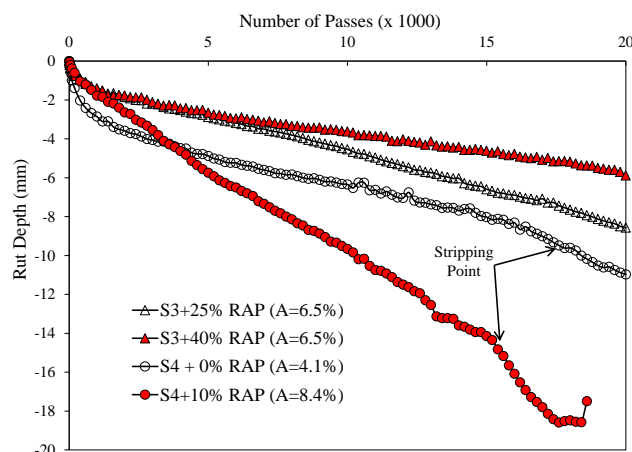


Fig. 7. Hamburg Curves of Mixes.

(9) to compute the stress, strain, and flexural stiffness per cycle as a function of the number of load cycles. In this study, fatigue life was defined as the number of repeated cycles corresponding to a 50 percent reduction in initial stiffness, which was measured at the 50th load cycle. The initial stiffness values and number of cycles to fatigue failure of beams determined by initial tensile stress and

**Table 3.** Summary of 4-point Beam Fatigue Tests.

Mix Type	% of RAP	Air Void (%)	Initial Stiffness (MPa)	Cycles to Failure ( $N_f$ )
S3	25%	4.2	7,039	670,000
S3	40%	4.4	8,981	4,925,000
S3	25%	5.9	5,467	840,000
S3	40%	6.4	7,795	2,433,333
S4	0%	3.8	5,729	279,071
S4	10%	7.1	4,231	367,095

strain are presented in Table 3.

It is evident from Table 3 that due to an increase in the RAP content in S3 mixes, the initial flexural stiffness and number of cycles to failure of beams increases. For example, at similar air void content of  $4.5 \pm 0.5\%$ , an increase in the RAP content from 25% to 40% increased initial stiffness by 28% (from 7,039 MPa to 8,981 MPa) and increased number of failure cycles from approximately 670,000 to 4,925,000 (635% increase). It is also evident from Table 3 that for S4 mix failure cycles increases with increase in RAP content (from 0% to 10%). On the contrary, initial stiffness value was found to decrease (from 5,729 MPa to 4,231 MPa) with increase in the RAP content for S4 mix. This could be attributed to relatively large difference (3.3%) in the air void content of S4 mixes. Xiao et al. [24] found no obvious trends for fatigue life and stiffness of HMA mixes as the RAP content increased.

## Conclusions

The present study described the design and construction of test section using RAP containing HMA. Further, the effect of RAP content on mechanistic performance of HMA mixes was evaluated by conducting creep compliance, dynamic modulus, Hamburg rut, and 4-point beam fatigue tests. Based on the results presented in this paper the following conclusions can be drawn:

- 1) The volumetric mix design results indicated that increase in the amount of RAP increased the VMA and VFA of the HMA mixes.
- 2) At higher reduced time (temperature  $> 0^\circ\text{C}$ ), mix containing lower amount of RAP (S3-25 or S4-0) exhibited higher creep compliance values as compared to high RAP containing (S3-40 or S4-10) mix at corresponding reduced time. Also, differences in creep values between mixes are more pronounced at higher reduced time or temperature.
- 3) Based on the results of Poisson's ratio, the S3 mix results, present an increase in Poisson's ratio values with an increase in the RAP content. On the other hand, the results of the S4 mixes show a decrease in Poisson's ratio values with an increase in the RAP content. However, the changes in the values of Poisson's ratio due to the RAP content of the HMA are not significant.
- 4) The test results of dynamic modulus, proposed as the key parameter in the new MEPDG, illustrated that the HMA mix containing higher amount of RAP has higher dynamic modulus values.

- 5) The increase in RAP content reduced rutting susceptibility of both S3 and S4 mixes. The moisture damage susceptibility of mixes was also found to improve with increase in RAP content.
- 6) At similar air void content, higher RAP containing S3 and S4 mixes showed longer fatigue life.

Overall, the present study indicated that the mix containing RAP will be more resistant to rutting, moisture damage and fatigue and less resistant to thermal cracking. However, it is recommended that similar studies be conducted for HMA mixes containing RAP and virgin aggregates and binder from different sources. Furthermore, performance of RAP containing mixes should also be evaluated in the field by collecting field data such as falling weight deflectometer, rutting measurements, and crack mapping.

## Acknowledgements

The authors are thankful to the Oklahoma Transportation Center (OkTC) and Oklahoma Department of Transportation (ODOT) for providing funds for this project. We would also like to acknowledge the assistance of Craig Parker, Clint Hurt, Mike Cooper, Jack Shannon, Charles Shawn and Terri A. Madden of Silver Star Construction Co. for the selection of RAP and construction of the test section with high RAP content. Finally, the assistance of students Curtis Doiron and Jackson Autrey of the University of Oklahoma are greatly appreciated.

## References

1. Federal Highway Administration (2012). *Asphalt Pavement Recycling with Reclaimed Asphalt Pavement (RAP)*, <http://www.fhwa.dot.gov/pavement/recycling/rap/index.cfm>, Last Accessed July 24, 2012.
2. Jones, C.L. (2008). Summit on Increasing RAP Use in Pavements State's Perspective, North Carolina Department of Transportation, presented at Moredap conference at Auburn, AL, USA.
3. Adje, D. (2012). Effect of Recycled Asphalt Pavement on Mechanistic Performance of Hot Mix Asphalt, Master's thesis, University of Oklahoma, Norman, OK, USA.
4. AASHTO (2004). Guide for Mechanistic-Empirical Design of New and Rehabilitated Pavement Structures. Final Report prepared for National Cooperative Highway Research Program (NCHRP), Transportation Research Board, National Research Council, Washington, DC, USA.
5. Daniel, J.S. and Lachance, A. (2005). Mechanistic and Volumetric Properties of Asphalt Mixtures with Recycled Asphalt Pavement. *Transportation Research Record*, No. 1929, pp. 28–36.
6. Richardson, D.N., and Lusher, S.M. (2008). Determination of creep compliance and tensile strength of Hot-Mix Asphalt for Wearing Courses in Missouri. *MoDOT Report OR08-18*, Missouri Department of Transportation, <http://library.modot.mo.gov/RDT/reports/Ri05052/or08018.pdf>, Last Accessed April, 2008.
7. McGraw, J., Johnson, E., Johnson, G., Dai, S., Linell, D., and Watson, M. (2010). Incorporation of Recycled Asphalt Singles

- in Hot-Mixed Asphalt Pavement Mixtures, *Report No. MN/RC 2010-08*, Minnesota Department of Transportation, St. Paul, MN, USA.
8. Loria, L., Hajj, E., Sebaaly, P., Barton, M., Kass, S., and Liske, T. (2011). Performance Evaluation of Asphalt Mixtures with High RAP Content. In *91<sup>st</sup> Annual Meeting of Transportation Research Board*, Washington, DC, USA.
  9. Bonaquist, R. (2011). *Characterization of Wisconsin Mixture Low Temperature Properties for the AASHTO Mechanistic-Empirical Pavement Design Guide. Final Report No. WHRP 11-12*, Wisconsin Department of Transportation, Madison, WI, USA.
  10. Rahman, F., Hossain, M., Hobson, C., and Schieber, G. (2012). Evaluation of Superpave Mixtures with High RAP Content. *Proceedings of GeoCongress 2012*, Oakland, CA, USA.
  11. Silva, H.M.R.D., Oliveira, J.R.M., and Jesus, C.M.G. (2012). Are Totally Recycled Hot Mix Asphalts a Sustainable Alternative for Road Paving? *Resources, Conservation and Recycling*, Vol. 60, pp. 38-48.
  12. Singh, D., Zaman, M., and Commuri, S. (2012). A Laboratory Investigation into the Effect of Long-Term Oven Aging on RAP Mixes Using Dynamic Modulus Test, *International Journal of Pavement Research and Technology*, 5(3), pp. 142-152.
  13. Christensen, D.W. (1998). Analysis of Creep Data for Indirect Tension Test on Asphalt Concrete, *Journal of the Association of Asphalt Paving Technologists*, Vol. 67, pp. 458 – 492.
  14. Bonaquist, R., and Christensen, D.W. (2005). Practical Procedure for Developing Dynamic Modulus Master Curves for Pavement Structural Design. *Transportation Research Record*, No. 1929, pp. 208-217.
  15. Oklahoma Department of Transportation (ODOT) (2010). *Construction Engineering, Material and Testing e-Guide*, Test Data, [www.okladot.state.ok.us/materials/tststatmu.htm](http://www.okladot.state.ok.us/materials/tststatmu.htm), Dec. 2010.
  16. Cooley, L. A., Jr., Kandhal, P.S., Buchanan, M.S., Fee, F., and Epps, A. (2000). Loaded Wheel Testers in the United States: State of the Practice. *Transportation Research E-Circular*, Number E-C016, TRB, National Research Council, Washington, DC, USA.
  17. Lu, Q. and Harvey, J.T. (2006). Evaluation of Hamburg Wheel-Tracking Device Test with Laboratory and Field Performance Data. *Transportation Research Record*, No. 1970, pp. 25 – 44.
  18. Yildirim, Y., Jayawickrama, P.W., Hossain, M.S., Alhabshi, A., Yildirim, C., Smit, A.F., and Little, D. (2007). Hamburg Wheel-Tracking Database Analysis. Final Report No. *FHWA/TX-05/0-1707-7*, Texas Department of Transportation, Austin, TX, USA.
  19. Izzo, R.P. and Tahmoressi, M. (1999). Use of Hamburg Wheel-Tracking Device for Evaluating Moisture Susceptibility of Hot-Mix Asphalt. *Transportation Research Record*, No. 1681, pp. 76-85.
  20. Williams, R.C. and Prowell, B.D. (1999). Comparison of Laboratory Wheel-Tracking Test Results with WesTrack Performance. *Transportation Research Record*, No. 1681, pp. 121-128.
  21. Stroup-Gardiner, M. and Wagner, C. (1999). Use of RAP in Superpave HMA Applications. *Transportation Research Record*, No. 1681, pp. 1-9.
  22. Li, X., Marasteanu, M.O., Williams, R.C., and Clyne, T.R. (2008). Effect of RAP (Proportion and Type) and Binder Grade on the Properties of Asphalt Mixtures. In *87<sup>th</sup> Annual Meeting of Transportation Research Board*, Washington, DC, USA.
  23. FHWA (2012). Turner-Fairbanks Highway Research Center Bituminous Mixtures Laboratory (BLM) web page. <http://www.fhwa.dot.gov/pavement/asphalt/labs/mixtures/hamburg.cfm>. Last Accessed July 24, 2012.
  24. Xiao, F., Amirkhanian, S.N., and Wu, B. (2011). Fatigue and Stiffness Evaluations of Reclaimed Asphalt Pavement in Hot Mix Asphalt Mixtures, *ASTM Journal of Testing and Evaluation*, 39(1), pp. 1-9.